

## Design of a pre-slit for SPring-8 undulator beamlines

S. Takahashi,\* Y. Sakurai and H. Kitamura

SPring-8, Kamigori, Ako-gun, Hyogo 678-12, Japan.  
E-mail: takahasi@sp8sun.spring8.or.jp

(Received 4 August 1997; accepted 28 October 1997)

A volumetric heating method is applied to the pre-slit placed on the SPring-8 standard-undulator beamline front ends in order to handle the very intensive photon beam. A graphite block is used as the radiation-absorbing body, which is brazed to a cooling holder made of oxygen-free high-conductivity copper. Various experiments and calculations have been carried out on the strength of the brazed joint. Comparisons between the experiments and calculations show that static fracture of the joint would not occur even under the highest heat load. The outgassing properties of the graphite blocks are also presented here.

**Keywords:** front ends; high-heat-load components; volumetric heating; vacuum properties of graphite.

### 1. Introduction

The pre-slit is one of the components on the front ends of the standard in-vacuum undulator beamlines at SPring-8, which absorbs the off-axis part of the photon beam so as to reduce the heat load on the front-end XY-slits assembly (Oura *et al.*, 1998) and the graphite filters assembly (Sakurai *et al.*, 1995). As the pre-slit is located at about 26.5 m from the undulator, it may receive a maximum normal-incidence peak power density of about  $550 \text{ W mm}^{-2}$ . To handle such high heat flux we have adopted a volumetric heating method, in which an isometric densified graphite block is used as a radiation-absorbing body. Fig. 1 shows a schematic drawing of the pre-slit assembly. The assembly includes four fixed masks installed in one vacuum chamber, each of which is composed of the radiation-absorbing body, having a different exit aperture size to those of the others, and a cooling holder, made of oxygen-free high-conductivity

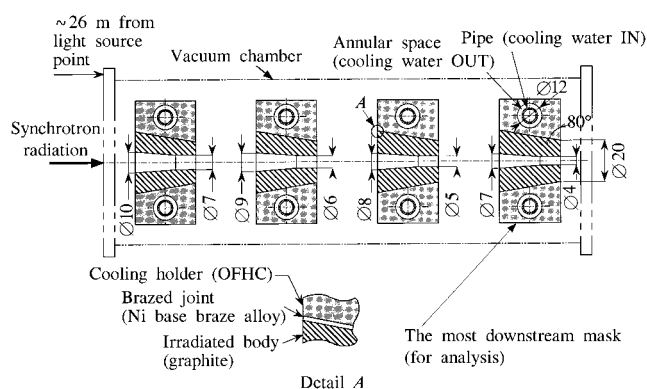


**Figure 1**  
Schematic drawing of the pre-slit assembly. Dimensions in millimetres unless otherwise stated.

copper (OFHC). The two materials are brazed together with a nickel-base braze alloy at about 1273 K. We present here the strength properties of the brazed joint and the outgassing properties of the graphite blocks.

### 2. Strength properties of the brazed joint

#### 2.1. Strength evaluation test

The test pieces for the static strength evaluation test have the same configuration and were brazed in the same way as the practical body. A load was applied in the axial direction onto the graphite portion while the OFHC holder is fixed; the load required to exfoliate the brazed joint was 17000 N on average, and exfoliation occurred at the graphite side of the joint in all cases.

A fatigue strength evaluation test was carried out in both tensile and shearing directions using an electro-hydraulic servo fatigue-testing machine. The test pieces were shaped in the general butt joint style. A 5 Hz sine-wave load was applied, and the stress ratio, namely the ratio of minimum stress ( $s_{\min}$ ) to maximum stress ( $s_{\max}$ ), was set at 0.1. We obtained the relationship between the stress amplitude  $[(s_{\max} - s_{\min})/2]$  and the cycles in both tensile and shearing directions. Concerning the shearing direction, the critical stress amplitude is about 98 MPa for a  $10^7$  cycle design life.

#### 2.2. Comparison of test results with analysis

An ANSYS finite-element analysis was performed on the most downstream mask, which is under the highest heat load. In the analytical model, the brazed joint gap was treated as an independent volume of metal nickel with a thickness of 0.05 mm. The analysis was carried out for the expected highest heat-flux case in normal operation, namely at a beam current of 100 mA and with a deflection parameter of the undulator ( $K$ ) of 2.3. Thermal analysis results show that the temperatures of the heated surface, cooling channel and brazed joint increase to 669, 335 and 352 K, respectively. Although there is no concern about the maximum

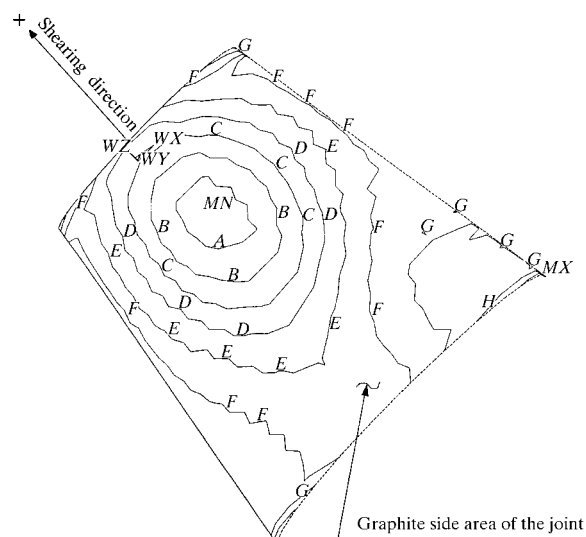


**Figure 2**  
Contour plot of the component stress distributions on nodes in the graphite side area of the joint in the shearing direction. Contour units ( $\text{kgf mm}^{-2}$ ): A, 2.857; B, 2.334; C, 1.811; D, 1.288; E, 0.765; F, 0.242; G, -0.281; H, -0.804.

temperatures, we have to pay attention to the resultant thermal stress generated on the brazed joint because of the different thermal expansion constraints. The calculated maximum thermal stress represented by Mizes's equivalent stress is 360 MPa on the brazed joint. The component stress distributions in the shearing direction on nodes in the graphite side area of the joint, where exfoliation of the joint occurred in the strength test, are shown in Fig. 2.

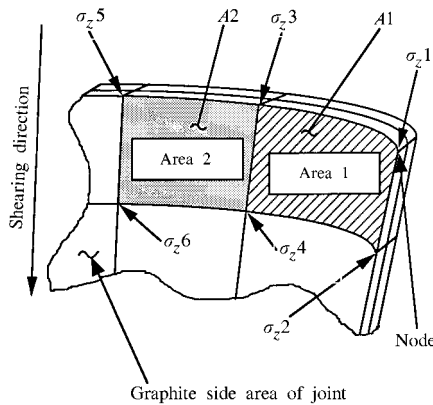
Summing up the component forces along the shearing direction on the graphite side joint (as shown in Fig. 3), we estimated the static force of the joint area generated by the thermal stress to be 14600 N. Comparing this estimated static force with the value of 17000 N obtained in the test, it is concluded that the fracture on the brazed joint in the shearing direction due to the thermal stress would not occur even at  $K = 2.3$ , the highest heat-load undulator operation.

**3. Outgassing properties of the graphite block**

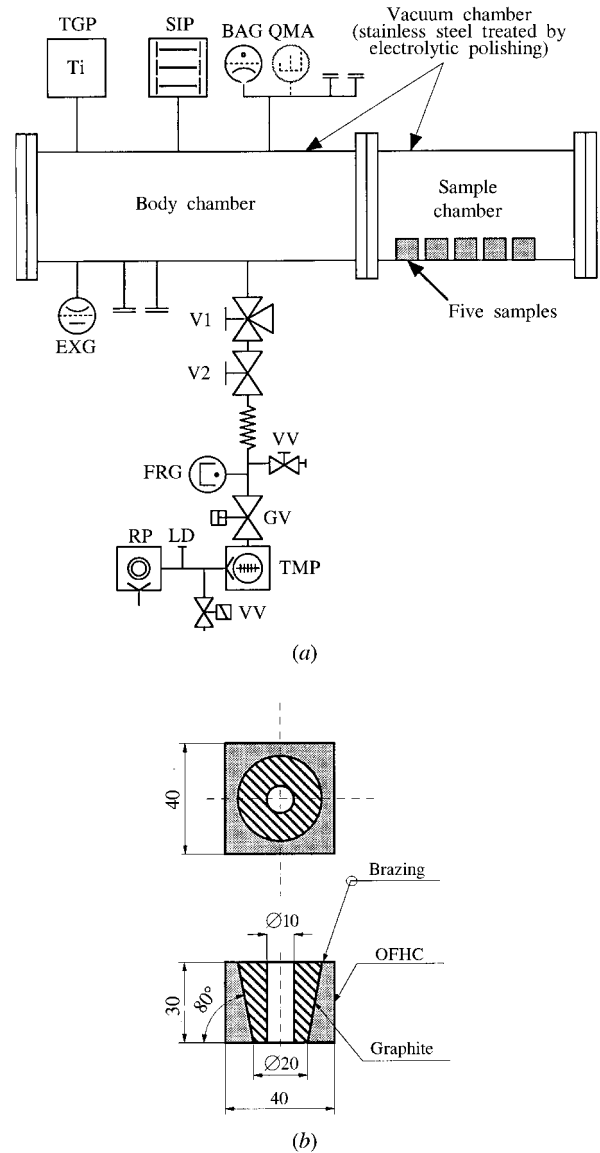
As graphite is essentially porous, we have undertaken a vacuum performance test on the graphite block using an ultra-high-vacuum test stand by comparing the pumping down performances and ultimate pressures of the test stand after bakeout with and without samples. Fig. 4 shows a schematic diagram of the test stand and details of the sample configuration. The pressure of the test stand was monitored by two kinds of gauges, namely a Bayard-Alpert nude gauge (BAG) and an extractor gauge (EXG). The samples were manufactured by the same procedure as those in practical use.

Fig. 5 shows the pumping down curves with and without samples after 523 K  $\times$  48 h bakeout. Considering the effect of dark current, the value of the BAG was revised by subtracting  $3 \times 10^{-9}$  Pa. The pressure for the case with samples was decreased to  $1.7 \times 10^{-9}$  Pa (EXG) or  $6.9 \times 10^{-9}$  Pa (BAG) in about 90 h after bakeout, when the ultimate pressure was observed in the case without samples. Continuing pumping at room temperature, the pressure decreased slowly but sometimes irregularly, and reached the base pressure in about 400 h after bakeout. Although the test stand is not of the type which can

measure the outgassing rate of a material quantitatively, we have estimated the outgassing rate of the graphite block. Assuming that (i) the outgassing rate of the chamber material (stainless steel treated by electrolytic polishing) is  $4.0 \times 10^{-9}$  Pa m<sup>3</sup> s<sup>-1</sup> m<sup>-2</sup>, which is equal to the value obtained when pumping at room temperature in about 24 h after 523 K  $\times$  30 h bakeout (Young, 1969), (ii) the outgassing rate of OFHC is less than that of stainless steel, and (iii) the difference in pressure with and without samples is due to the thermal outgassing of the graphite blocks, then the outgassing rate of the graphite blocks is estimated to be  $8.5 \times 10^{-11}$ – $1.4 \times 10^{-10}$  Pa m<sup>3</sup> s<sup>-1</sup> m<sup>-2</sup> when pumping at room temperature in about 180 h after 573 K  $\times$  48 h bakeout.



**Figure 3**  
Summing up the component forces along the shearing direction on the graphite side area of the joint using the component stress on each node.  $P_{ana1} = A1(\sigma_z1 + \sigma_z2 + \sigma_z3 + \sigma_z4/4)$ ,  $P_{ana2} = A2(\sigma_z3 + \sigma_z4 + \sigma_z5 + \sigma_z6/4)$  etc.,  $TP_{ana} = \Sigma P_{ana}$ , where  $\sigma_z$  is the component stress in the shearing direction on each node,  $A$  is the area of each element,  $P_{ana}$  is a real static force in the shearing direction in each element, and  $TP_{ana}$  is the total static force in the shearing direction throughout the graphite side area of the joint.



**Figure 4**  
(a) Schematic diagram of the ultra-high-vacuum test stand. Vacuum chamber area: 13000 cm<sup>2</sup> (stainless steel). Sample area: OFHC, 69.5 cm<sup>2</sup>  $\times$  5 pieces; graphite, 18.3 cm<sup>2</sup>  $\times$  5 pieces. V1, all metal valve; V2, viton valve; GV, gate valve; VV, vent valve; TMP, turbo molecular pump; RP, rotary pump; TGP, titanium getter pump; SIP, sputter ion pump; BAG, Bayard-Alpert nude gauge; EXG, extractor gauge; FRG, full range gauge (Pirani gauge + cold cathode gauge); LD, leak detector; QMA, quadrupole mass spectrometer. (b) Details of the sample configuration.

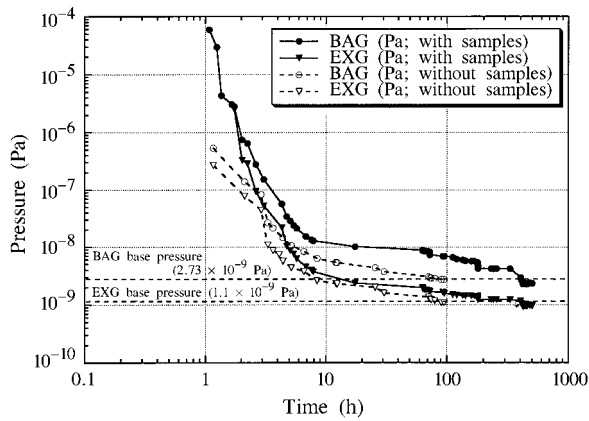


**Figure 5**

Pumping curves measured by BAG and EXG after  $573\text{ K} \times 48\text{ h}$  bakeout with and without samples.

#### 4. Conclusions

We have carried out various evaluation tests and analyses on the strength of the brazed joint. Furthermore, the outgassing properties of the graphite blocks were also investigated. Conse-

quently, the static fracture of the brazed joint would not occur even under the highest-heat-load in-vacuum standard undulator operation, and the isometric densified graphite can be used as a structural material on SPring-8 front ends. However, from the point of view of the fatigue strength and the outgassing performance, further development is still necessary. We have just started the feasibility study of the application of beryllium blocks as synchrotron radiation absorption material instead of graphite.

The authors wish to acknowledge the support of Dr Takashi Tanaka of JASRI during construction and operation of the ultra-high-vacuum test stand.

#### References

- Oura, M., Sakurai, Y. & Kitamura, H. (1998). *J. Synchrotron Rad.* **5**, 606–608.
- Sakurai, Y., Oura, M., Sakae, H., Usui, T., Kimura, H., Oikawa, Y., Kitamura, H., Konishi, T., Shiwaku, H., Nakamura, A., Amamoto, H. & Harami, T. (1995). *Rev. Sci. Instrum.* **66**, 1771–1773.
- Young, J. R. (1969). *J. Vac. Sci. Technol.* **6**, 398.